Journal of Applied Pharmaceutical Science Vol. 14(12), pp 090-097, December, 2024
Available online at http://www.japsonline.com
DOI: 10.7324/JAPS.2024.177392
ISSN 2231-3354

Flavonoid compound of red fruit papua and it derivatives against sars-cov-2 mpro: An *in silico* approach

Agus Dwi Ananto[1,2], Harno Dwi Pranowo[1*], Winarto Haryadi[1], Niko Prasetyo[1]

[1]Department of Chemistry, Faculty of Mathematics and Natural Sciences Universitas Gadjah Mada, Yogyakarta, Indonesia.
[2]Department of Pharmacy, Faculty of Medicine and Health Science, Universitas Mataram, Mataram, Indonesia.

ARTICLE HISTORY

Received on: 14/05/2024
Accepted on: 15/09/2024
Available Online: 05/11/2024

Key words:
Docking, MD simulation, pharmacokinetic profile, SARS-CoV2 Mpro, herbal medicine.

ABSTRACT

In the past years, the world has experienced a profound impact due to the abrupt appearance of a new virus (COVID-19), presenting a significant threat to human health. Currently, there exists no widely established treatment for COVID-19 that proves consistently effective, but many studies have implemented drug repurposing and the use of herbal medicines. The potential of antiviral compounds from natural products can be predicted through *in silico* approach. This study aimed to determine and design flavonoid compounds from red fruits and their derivatives that have the potential to suppress the SARS-CoV-2 Mpro, ensuring a stable molecular framework and adhering to a standard pharmacokinetic profile. The study started with molecular docking using a lead compound followed by Molecular dynamics (MD) simulation up to 100 ns and pharmacokinetic prediction. The analysis of docking outcomes reveals that among flavonoid compounds, quercetin 3'-glucoside exhibits the most favorable binding energy value. Furthermore, the identification of hydrogen bonds with amino acid residues Asn142 and Cys145 provides additional rationale for selecting this compound as a pivotal candidate in the design of novel derivatives. The molecular docking procedure and subsequent MD simulations were conducted utilizing the Yasara-structure software. Furthermore, the evaluation of the pharmacokinetic profile was performed utilizing pkCSM ADMET to gain insights into the compound's absorption, distribution, metabolism, excretion, and toxicity characteristics. According to the docking outcomes, among the 225 newly designed compounds, the ligand with code SR133 demonstrated the most favorable binding energy of −8.0950 Kcal/mol, surpassing the reference compound. Subsequent MD simulation analysis indicates that this ligand demonstrates good stability. The presence of hydrogen bonds in the active site of SARS-CoV-2Mpro involving the main amino acid residues Asn142 and Cys145 further clarifies that this new compound has excellent inhibitory potential. The pharmacokinetic prediction of SR133 shows that this compound has a good pharmacokinetic profile and is worth proposing as a new drug candidate.

INTRODUCTION

Indonesia is a rich country in natural resources. Almost all plants that grow on earth can be found in Indonesia [1]. Numerous plants exhibit efficacy as herbal medicines. Herbal medicine also plays an important role in controlling infectious diseases. One of the infectious diseases that has become a global concern in the past 2 years is COVID-19. The handling efforts carried out by both WHO and the Government of Indonesia are to promote vaccination. Massive vaccination efforts have been able to reduce the prevalence of COVID-19 sufferers [2,3]. Even with a noticeable recent decline, COVID-19 continues to exhibit elevated prevalence and mortality rates, further accentuated by the lack of a verified, effective treatment. WHO also reported 1,009,341 COVID-19 cases in the last 28 days until December 24, 2023, an increase of 467,261 cases from the previous period [4]. This emphasizes the crucial need for rigorous and all-encompassing medical strategies to confront the virus.

In vitro, investigations have highlighted the potent inhibition of SARS-CoV-2 infection by both Favipiravir and Remdesivir in standard Vero E6 cells [5]. Multiple studies have assessed various antiviral medications on SARS-CoV-2

*Corresponding Author
Harno Dwi Pranowo, Department of Chemistry, Faculty of Mathematics and Natural Sciences Universitas Gadjah Mada, Yogyakarta, Indonesia.
E-mail: harnodp@ugm.ac.id

patients, such as hydroxychloroquine [6], Lopinavir-Ritonavir, and Ribavirin [7], Remdesivir [8], and Tocilizumab [9]. The FDA in the United States has granted authorization for the use of Nirmatrelvir and Ritonavir (Paxlovid) as a treatment for mild to moderate COVID-19 in both adults and children [10].

Other than the use of synthetic drugs, there is clinical evidence that herbal plants can be used as an alternative therapy for SARS-CoV-2. [11,12]12]. Indonesia also contributes a variety of herbal plants, one of them is the red fruit plant (*Pandanus conoideus* Lamk) that can inhibit SARS-CoV-2. Red fruit is a typical plant from Papua, Indonesia. Red fruit contains antioxidants, antitumor, immunomodulator, antiparasitic, and anti-HIV [13,14,15]. Previous research reported that flavonoid compounds contained in red fruit have the potential to an anti-SARS-CoV-2 Mpro. The hydrogen bonds formed on the main protease active sites of SARS-CoV-2 Mpro are Asn142 and Cys145 [16].

The potency of antiviral compounds from herbal plants can be predicted through *in silico* method. This approach enables a quick and precise selection of various compounds. In addition, this approach can also save time and money when compared to the conventional drug discovery stage. Moreover, for the COVID-19 antiviral test, a minimum laboratory standard of Biosafety Level 3 (BSL-3) is required [17]. The molecular docking method approach can be used to design or select compounds that act precisely on target proteins and observe the mechanism of action of these compounds molecularly [18]. This method allows researchers to determine the anti-COVID-19 activity by looking at the binding energy value of the compound's ability to bind the receptor and the compound engages with the amino acid residues on the target receptor through a specific type of bond [19]. By studying the dynamics of systems in the body, Molecular dynamics (MD) simulations can reveal the ligand-protein's stability complex [20,21,21,22]21,22].

The stability of ligand-protein complexes in the body is just one aspect of research in the identification of new substances with therapeutic capabilities. In addition, the pharmacokinetic characteristics of these drugs should still be considered. The pharmacokinetic profile of a substance can be seen by estimating its absorption, distribution, metabolism, excretion, and toxicity (ADMET) [23].

Therefore, based on all of the reasons above, this study's aim is to determine and design flavonoid compounds found in red fruit, and the derivatives that possess the potential to inhibit SARS-CoV-2 Mpro with a stable structure and standard pharmacokinetic profile. The study started with molecular docking followed by MD simulation up to 100 ns and pharmacokinetic prediction.

MATERIAL AND METHODS

Materials

The main instrument employed in this study was a PC with an Intel Core i7-13700KF CPU, and 64 GB of RAM. The OS utilized is Linux, and the primary software installed is Yasara-Structure 23.8.19 [24], Discovery Studio Visualizer (DSV) 21.1.0.20298 [25]. All software settings were left at their default values. Materials utilized include the SARS-CoV-2Mpro crystal structure with PDB ID: 5r7y [26].

Methods

The structural data for the SARS-CoV-2 main protease (PDB ID: 5r7y) was sourced from the protein data bank [26]. This structure underwent a preparation phase involving the removal of water molecules and ions using Yasara-structure tools. While the native ligand, JFM (N-(2-phenylethyl) methanesulfonamide), remained for benchmarking the potential of herbal bioactive compounds as competitors, water molecules, and ions were eliminated. To validate the docking methodology, 100 redocking iterations of the native ligand were conducted utilizing supplementary plug-ins within the Yasara-structure.

There have been 225 compound modifications performed. Each compound design of quercetin 3'-glucoside derivatives can be seen in Supplementary Table 1. Figure 1 depicts the lead compound of quercetin 3'-glucoside. Preparation begins with the separation of the protein and its native ligand. The next stage of preparation produces *5r7y_receptor.sce* and *5r7y_ligand.yob* files. All compound modification changes were energy-reduced, before moving on to the molecular docking stage.

Molecular docking

Yasara-structure, employing a force field scoring function approach, serves as the basis for the docking method utilized to calculate the binding energy value. The docking process is performed using macro command (*dock_run.mcr*) which is available in Yasara-structure. The grid box was created with a radius of 5.0 Å around the native ligand. The Vina docking method within the Yasara-structure was utilized to compute binding energy and identify receptor residues involved in the interaction. Upon finishing the docking process, the outcomes were stored in the PDB (.pdb) file format. Subsequently, the post-docking data underwent analysis and visualization using DSV [25].

MD simulation

Yasara-structure was employed for conducting molecular dynamics simulations on a Linux system, leveraging the *md_runmembrane.mcr* macro command for preparation, minimization, equilibration, and production phases. During the preparation phase, crucial parameters encompassed a cubic simulation cell containing water solvent, cell configuration with periodic boundaries, a membrane box size 30 Å larger than the protein, and a water box size 20 Å larger than the protein. Additionally, 0.9% NaCl ions were introduced, employing the AMBER14 forcefield. The simulation was set at pH 7.4, a temperature of 300 K, and a pressure of 1 bar [27,28]28]. Executed at a speed of 2.5 fs, the simulation data were automatically saved in *.sim* file format, lasting for 100 ns. Post-simulation, the *md_analyze.mcr* macro command in Yasara-structure was utilized for determining RMSD and RMSF values, while the *BEcalculation.mcr* macro command evaluated the binding free energy from the MD simulation results.

Table 1. Binding energy value and contacting receptor residue from docking result.

No	Ligand	Binding energy (Kcal/mol)	Contacting receptor residues
1	4′,6,6′,8-tetrahydroxy-3-methoxy-flavon	−7.0620	A THR24 A THR25 A HIS41 A CYS44 A THR45 A SER46 A MET49 A ASN142 A GLY143 A CYS145 A HIS164 A MET165 A GLU166 A LEU167 A ARG188 A GLN189
2	3,4′,5-trihydroxy-7,3′-dimethoxy flavon	−7.0170	A THR24 A THR25 A THR26 A LEU27 A HIS41 A CYS44 A THR45 A SER46 A MET49 A LEU141 A ASN142 A GLY143 A CYS145 A HIS163 A HIS164 A MET165 A GLU166
3	Taxifolin 3-O-α-arabinopyranose	−7.2700	A THR25 A THR26 A LEU27 A HIS41 A VAL42 A CYS44 A THR45 A SER46 A MET49 A ASN142 A GLY143 A CYS145 A MET165 A GLU166 A ASP187 A ARG188 A GLN189
4	Quercetin 3-O-glucose	−7.8410	A THR25 A THR26 A LEU27 A HIS41 A CYS44 A THR45 A SER46 A MET49 A ASN142 A GLY143 A CYS145 A MET165 A GLU166 A ARG188 A GLN189 A THR190
5	Quercetin 3-methyl-ether	−7.2820	A THR25 A HIS41 A CYS44 A THR45 A SER46 A MET49 A ASN142 A GLY143 A CYS45 A HIS163 A MET165 A GLU166 A ARG188 A GLN189 A GLN192
6	Quercetin	−7.3950	A THR25 A HIS41 A VAL42 A CYS44 A THR45 A SER46 A MET49 A ASN142 A GLY143 A CYS145 A HIS163 A HIS164 A MET165 A GLU166 A ARG188 A GLN189 A THR190
7	Taxifolin	−7.1040	A THR25 A HIS41 A CYS44 A THR45 A SER46 A MET49 A ASN142 A GLY143 A CYS145 A HIS163 A HIS164 A MET165 A GLU166 A ARG188 A GLN189 A THR190
8	Quercetin 3′-glucoside	−8.0950	A THR24 A THR25 A THR26 A HIS41 A CYS44 A THR45 A SER46 A MET49 A PHE140 A LEU141 A ASN142 A GLY143 A SER144 A CYS145 A HIS163 A HIS164 A MET165 A GLU166 A HIS172 A ASP187 A GLN189
9	Ligand native	−4.8710	A THR24 A THR25 A THR26 A LEU27 A HIS41 A CYS44 A THR45 A SER46 A MET49 A GLY143 A CYS145
10	Remdesivir	−7.5200	A THR25 A LEU27 A HIS41 A CYS44 A THR45 A SER46 A MET49 A ASN142 A CYS145 A HIS163 A HIS164 A MET165 A GLU166 A LEU167 A PRO168 A ASP187 A GLN189 A THR190
11	Paxlovid	−7.3450	A THR24 A THR25 A THR26 A LEU27 A HIS41 A CYS44 A THR45 A SER46 A MET49 A ASN142 A GLY143 A CYS145 A HIS164 A MET165 A GLU166 A ASP187 A GLN189
12	SR133	−8.3370	A THR24 A THR25 A THR26 A LEU27 A HIS41 A CYS44 A THR45 A SER46 A MET49 A ASN142 A GLY143 A CYS145 A HIS163 A HIS164 A MET165 A GLU166 A LEU167 A PRO168 A ARG188 A GLN189 A THR190 A GLN192

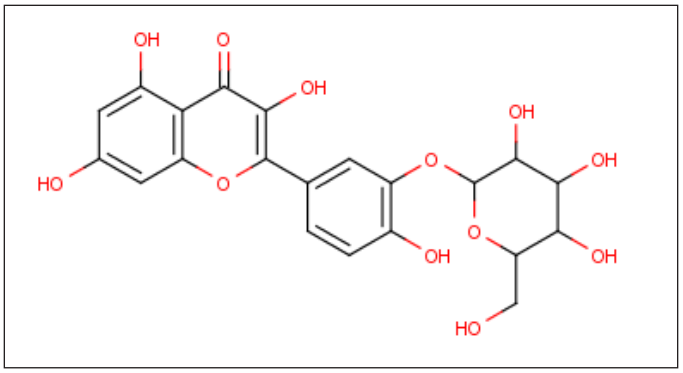

Figure 1. Lead compound of quercetin 3’-glucoside.

The molecular dynamics analysis revealed the binding free energy to be exceptionally stable, subsequently undergoing rigorous internal validation. This validation process encompassed an extensive assessment conducted across 1,000 redocking iterations, enabling a comparison of docked postures for the calculation of RMSD values concerning the docked ligand poses [27,28]28]. The first step in this redocking process involves using the *target_prep.mcr* macro command to dissociate the protein from the ligand. Subsequently, the redocking procedure can be iteratively repeated 1,000 times using the *dock_run_1,000.mcr* macro command. The RMSD value obtained can be used to determine the outcome of this validation.

Pharmakokinetic prediction

pkCSM ADMET was utilized to forecast the pharmacokinetic profiles of selected ligands, evaluating both the quality and safety of these compounds. The generation of SMILES strings for each ligand involved the conversion of PDB ligand files into SMI format using DSV, enabling comprehensive analysis.

RESULTS AND DISCUSSION

Molecular docking

Molecular docking can predict the structure of ligand-protein complexes. Docking simulations can illustrate how a drug candidate attaches to its target protein to determine its potential affinity and activity [29]. As an outcome of this docking simulation, the docking score was utilized to gauge the binding energy value, reflecting the strength of interaction between the ligand and the receptor [30].

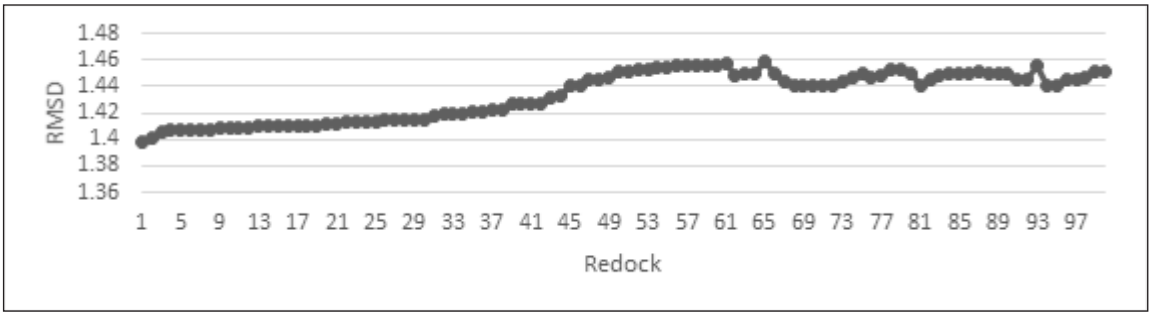

Figure 2. RMSD value for redocking 100 times.

The crystal structure with PDB ID 5r7y is employed as the target for the SARS-CoV-2 Mpro due to scientific evidence indicating that compounds interacting with this protein hold potential as antiviral agents. As a crucial component of SARS-CoV-2 Mpro, the 5r7y protein serves as a significant focus in the quest for antiviral drug development against the virus. Through computational analyses and laboratory investigations, compounds exhibiting strong binding affinity to the 5r7y protein have demonstrated inhibitory effects against SARS-CoV-2 Mpro, presenting themselves as promising candidates for combating SARS-CoV-2 infection. Scientific research underscores the pivotal role of the 5r7y protein in the replication cycle of the SARS-CoV-2 virus, thus inhibiting its activity holds the potential to impede viral development. Consequently, leveraging the 5r7y protein as a target for inhibiting SARS-CoV-2 Mpro represents a promising strategy in the endeavor to develop antiviral medications to combat COVID-19 [26,31].

Based on Supplementary Table 1, design of new compound is intended to increase the value of the docking score, binding energy, and contact with receptor residue. The substituting groups are electron-donating and electron-withdrawing groups. Furthermore, the reason for using the groups is also based on the substitution of isosteres groups. This is done because the substitution of isosteres groups can increase the resulting docking score of the ligand-protein complex [32].

The validation of the docking methodology involved 100 times redocking against the native ligand. This validation method produced a delta RMSD value of less than 1.5 (Fig. 2). Therefore, the docking method to be used is proven to be valid.

After the docking approach was determined to be valid, the next step was to dock all flavonoid compounds discovered in red fruit. In addition, we employed remdesivir and paxlovid as positive controls. The binding energy value of flavonoid compounds from the best docking results is then used as a lead compound to design new compounds. Table 1 displays the binding energy and contacting receptor residue values for red fruit flavonoids, remdesivir, paxlovid, and the design of a new compound derivative of quercetin 3′-glucoside as the best docking results.

Based on the docking results of flavonoid compounds found in red fruit, the quercetin 3′-glucoside compound had the highest binding energy value. This follows the previous research which declares that flavonoid (quercetin 3′-glucoside) has the potential to inhibit SARS-CoV-2 Mpro [16]. Therefore,

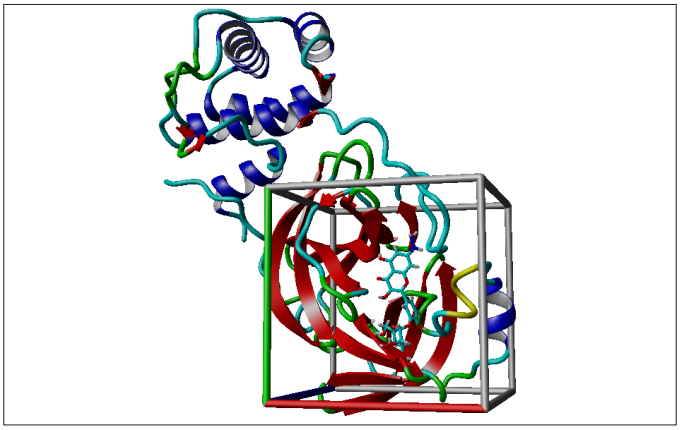

Figure 3. Docking for SR133 results.

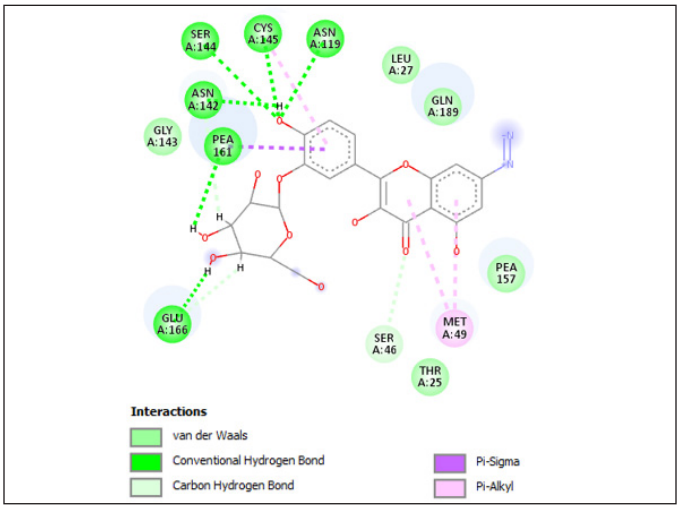

Figure 4. The visualization of the ligan-protein complex after MD simulation.

we further used this compound as a lead compound in designing new compounds. A total of 225 proposed compounds were docked showing that the design compound with code number 133 (SR133) had a better binding energy value than the native ligand, lead compound, or reference ligands (remdesivir and paxlovid) (Fig. 3). This docking stage uses 999 iterations of each ligand (Table 1). Based on the table, it can be seen that SR133 has a better binding energy value than other ligands. The

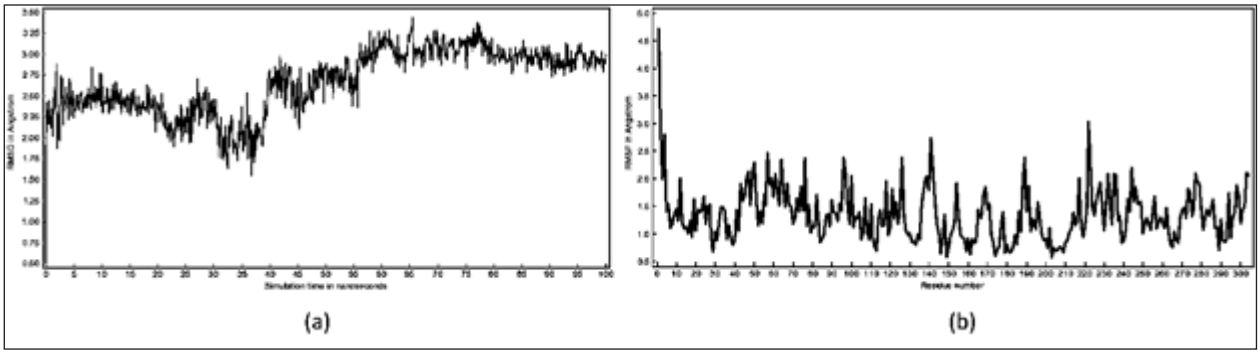

Figure 5. (a) RMSD (Å) vs time (ns) relationship graph; (b) RMSF vs residue number relationship graph.

free binding energy of the complex is −8.3370 Kcal/mol. This table also provides a visual representation of the contacting receptor residues between ligands and proteins.

MD simulation

The ligand-protein complex's stability can be determined via MD simulation. The MD simulation data was subsequently employed to calculate both the RMSD and free-binding energy values. Figure 4 illustrates the visualization of the ligand-protein complex. The authors chose to conduct molecular dynamic simulations at 300 K because this temperature is commonly used in MD simulations to represent room temperature, and it allows for comparison with a wide range of other studies. The impact of this temperature on their results is important to consider, as it may affect the conformational space sampled by the protein and the stability of the system. While enzymes are bioactive at body temperature (~310 K), the use of 300 K is often justified by the fact that the conformational space sampled by the protein is not significantly different from that at 310 K. The thermal equilibrium reached at 300 K ensures a consistent kinetic energy distribution, crucial for accurately representing system behavior. Moreover, simulating at this temperature facilitates direct comparison with experimental data, enhancing validation and interpretation of simulation outcomes, especially in fields where experiments are commonly conducted at or around room temperature [33,34]34]. Furthermore, simulations conducted at elevated temperatures were prevalent in the early stages of MD development, yet they resulted in unrealistic trajectories, highlighting the need for their integration with runs performed at room temperature [35].

The visual representation highlights the presence of crucial hydrogen bonds with key amino acid residues (Asn142 and Cys145), essential for inhibiting SARS-CoV-2 Mpro. Prior research has emphasized that the active site of SARS-CoV-2 Mpro encompasses hydrogen bonds specifically with the primary amino acid residues Asn142 and Cys145 [36]. Furthermore, there exist supplementary hydrogen bonds involving Asn119, Ser144, Pea161, and Glu166 collectively contributing to an augmented potential for inhibiting this virus.

The MD simulation findings indicated stabilization of the RMSD value after 2 ns. Calculations of the delta RMSD value were conducted every 5 ns, consistently yielding values less than 1 Å (Fig. 5a). Moreover, the system exhibited a free binding energy value of −5.7040 Kcal/mol, signifying the most

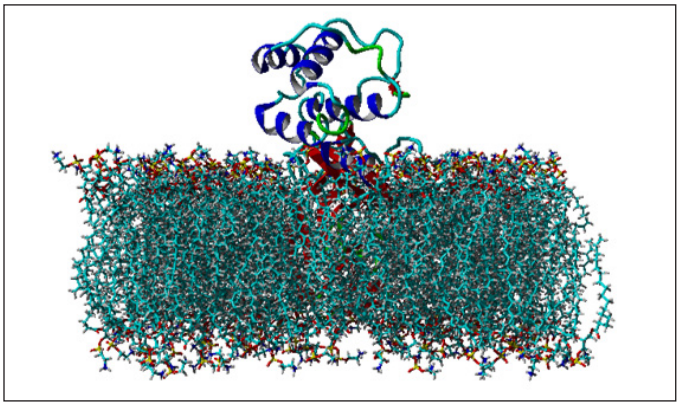

Figure 6. The system with the highest level of stability.

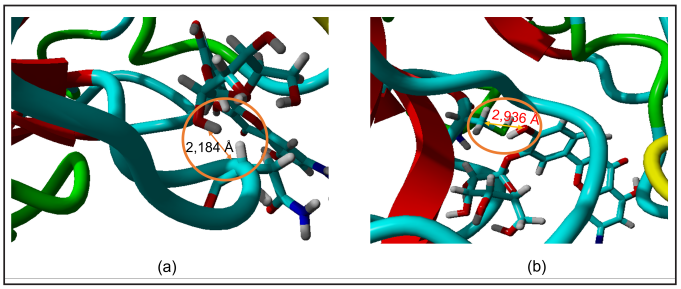

Figure 7. (a) Interaction between SR133 and Asn142. (b) Interaction between SR133 and Cys145.

stable during the computation of binding free energy (Fig. 6). According to thermodynamics, if a ligand-receptor complex was formed that has a lower potential energy, then interconnection between the ligand and the receptor can occur [37].

The experiment was subsequently expanded to include measuring the RMSF values of amino acid residues. This described the interaction's stability throughout the simulation, as measured at each residue position based on the fluctuations that occur. Figure 5b illustrates a graphical depiction of the correlation between the RMSF value and the corresponding residue number. Amino acid residue fluctuations occur as a result of ligand-induced binding, where increased fluctuation values indicate increased residue flexibility and thus indicate

Table 2. ADMET prediction of SR133.

Property	Name of model	Predictive value	Unit
Absorption	Solubility in water	−3.386	Numerical (log mol/l)
	Permeability of Caco2	−0.521	Numerical (log Papp in 10–6 cm/s)
	Intestinal absorption (human)	37.849	Numerical (% Absorbed)
	Skin permeability	−2.763	Numerical (log Kp)
	P-glycoprotein substrate	Yes	Category (Yes/No)
	P-glycoprotein I inhibitor	Yes	Category (Yes/No)
	P-glycoprotein II inhibitor	No	Category (Yes/No)
Distribution	VDss (human)	−1.44	Numerical (log L/kg)
	Fraction unbound (human)	0.419	Numerical (Fu)
	BBB permeability	−1.617	Numerical (log BB)
	CNS permeability	−4.256	Numerical (log PS)
Metabolism	CYP2D6 substrate	No	Category (Yes/No)
	CYP3A4 substrate	Yes	Category (Yes/No)
	CYP1A2 inhibitior	No	Category (Yes/No)
	CYP2C19 inhibitior	No	Category (Yes/No)
	CYP2C9 inhibitior	No	Category (Yes/No)
	CYP2D6 inhibitior	No	Category (Yes/No)
	CYP3A4 inhibitior	No	Category (Yes/No)
Excretion	Total clearance	0.462	Numerical (log ml/min/kg)
	Renal OCT2 substrate	No	Category (Yes/No)
Toxicity	AMES toxicity	No	Category (Yes/No)
	Max. tolerated dose (human)	0.597	Numerical (log mg/kg/day)
	hERG I inhibitor	No	Category (Yes/No)
	hERG II inhibitor	Yes	Category (Yes/No)
	Oral rat acute toxicity (LD50)	2.225	Numerical (mol/kg)
	Oral rat chronic toxicity (LOAEL)	2.121	Numerical (log mg/kg_bw/day)
	Hepatotoxicity	No	Category (Yes/No)
	Skin sensitisation	No	Category (Yes/No)
	T.Pyriformis toxicity	0.285	Numerical (log ug/l)
	Minnow toxicity	4.033	Numerical (log mM)

reduced stability in the amino acid residue interactions formed [38]. The suggested ligand demonstrated high interaction stability within the main catalytic site of SARS-CoV-2Mpro, evident from its low RMSF values.

During the visual analysis of the MD simulation report, hydrogen bonds were observed forming between the ligand's H atom and Asn142 residue, as well as between the ligand's O atom and Cys145. The calculated bond distances were 2.184 Å and 2.936 Å, respectively (Fig. 7). According to the criteria where a donor and/or acceptor within ≤3.5 Å indicate potential hydrogen bond formation [39], these interactions were noted. Consequently, this system was purposefully chosen and meticulously examined for validation. By conducting internal validation through 1,000 ligand-receptor redocking iterations, each with 25 iterations, a comprehensive set of 1,000 datasets featuring RMSD values under 2 Å was generated. The detailed RMSD values for these datasets are available in Supplementary Table 2.

Pharmacokinetics prediction

The best-suggested chemical has undergone pharmacokinetic prediction, and the outcome was ADMET prediction for the SR133 ligand (Table 2). Based on their solubility properties, drugs can be categorized as follows. A drug has high solubility if its LogS value is greater than −2, slightly soluble between −2 and −4, and insoluble below −4. SR133 has good solubility, as seen from the findings of the ADMET prediction study. The potent ligand exhibited strong oral absorption and skin penetration, as identified by HIA values >30% and Log Kp for skin permeability < −2.5. In addition, the ligand was not registered as a P-glycoprotein II inhibitor [40].

Ligand distribution was excellent when the log Vdss value was −1.44 log l/kg and the plasma's free fraction exceeded 20%. The higher the free fraction, the higher the medicine's effectiveness, requiring a reduced amount of drug per dosage. Additionally, the ligand only barely penetrated the blood barrier (logBB < −1 and logPS < −3), suggesting that it will not have direct impacts on the central nervous system. It may be claimed that the ligand does not interact with the metabolism of other medications because it neither acts as a substrate nor inhibits cytochrome P450 [27]. SR133 has a total clearance of 0.462, and the ligand is not an OCT2 substrate. The maximum SR133 dosage that is tolerated for humans is 0.597 log mg/kg/day. Table 2 also displays the ligand's acute and long-term toxicity to rats when administered orally. The ligand was non-irritating and non-hepatotoxic.

CONCLUSION

The molecular docking results of flavonoid compounds from red fruit reveal that quercetin 3'-glucoside exhibits the highest binding energy value of −8.0950 Kcal/mol. Additionally, this compound interacts with critical receptor residues, such as Asn142 and Cys145 located in the active site of the SARS-CoV-2 Mpro, further justifying its selection as a lead compound for designing novel derivatives. Moreover, a successful design process has yielded a total of 225 new compounds. Based on molecular docking results, molecular dynamics simulation, and pharmacokinetic prediction, it is evident that quercetin 3′-glucoside derivatives [7-diazenyl-3,5-dihydroxy-2-(4-hydroxy-3-{(3,4,5-trihydroxy-6-(hydroxymethyl)oxan-2-yl)oxy}phenyl)-4H-chromen-4-one], show considerable promise as SARS-CoV-2Mpro inhibitors. The docking result reveals that this novel compound exhibits the highest binding energy value of −8.3370 kcal/mol. Additionally, it forms hydrogen bonds with key amino acid residues, namely Asn142 and Cys145. Molecular dynamic

simulations further confirm the stability of its structure. Moreover, the pharmacokinetic evaluation indicates that this compound possesses a favorable adsorption, distribution, metabolism, excretion, and toxicity profile, positioning it as a promising candidate for drug development.

ACKNOWLEDGEMENTS

The Authors acknowledge the scholarship provided by "Indonesia Endowment Funds for Education (LPDP) and Center for Higher Education Funding (BPPT)", and gratefully acknowledge all research facilities provided by the Austrian-Indonesian Center for Computational Chemistry, Department of Chemistry, Faculty of Mathematics and Natural Sciences Universitas Gadjah Mada. This study was supported by Final Project Recognition Grant Universitas Gadjah Mada Number 5075/UN1.P.II/Dit-Lit/PT.01.01/2023.

AUTHOR CONTRIBUTIONS

All authors made substantial contributions to and design, acquisition of data, or analysis interpretation of data; took part in drafting the article or revising it critically for important intellectual content; agreed to submit to the current journal; gave final approval of the version to be published; and agree to be accountable for all aspects of the work. All the authors are eligible to be an author as per the the international committee of medical journal editors (ICMJE) requirements/ guidelines.

CONFLICTS OF INTEREST

The authors report no financial or any other conflicts of interest in this work.

ETHICAL APPROVALS

This study does not involve experiments on animals or human subjects.

DATA AVAILABILITY

All the data is available with the authors and shall be provided upon request.

USE OF ARTIFICIAL INTELLIGENCE (AI)-ASSISTED TECHNOLOGY

The authors declares that they have not used artificial intelligence (AI)-tools for writing and editing of the manuscript, and no images were manipulated using AI.

PUBLISHER'S NOTE

This journal remains neutral with regard to jurisdictional claims in published institutional affiliation.

REFERENCES

1. Minister of Health of the Republic of Indonesia Number: 381 concerning the 2007 National Traditional Medicine Policy, Jakarta, Indonesia: Minister of Health.
2. Covid19.go.id [Internet]. Indonesia: Covid-19 response task force, Situasi COVID-19 di Indonesia. [updated 2023 Jun 27; cited 2023 Jul 15]. Available from https://covid19.go.id/id/
3. Covid19.who.int [Internet]. World Health Organization: WHO Coronavirus (Covid-19) Dashboard, [cited 2023 August 4]. Available from https://covid19.who.int/
4. Data.who.int [Internet]. WHO Coronavirus (COVID-19) dashboard > Cases [Dashboard], [cited 2024 Jan 2]. Available from https://data.who.int/dashboards/covid19/cases
5. Wang M, Cao R, Zhang L, Yang X, Liu J, Xu M, *et al.* Remdesivir and chloroquine effectively inhibit the recently emerged novel coronavirus (2019-nCoV) *in vitro*. Cell Res. 2020;30:269–71.
6. Mahévas M, Tran VT, Roumier M, Chabrol A, Paule R, Guillaud C, *et al.* Clinical efficacy of hydroxychloroquine in patients with covid-19 pneumonia who require oxygen: observational comparative study using routine care data. BMJ. 2020;369:m1844.
7. Hung IFN, Lung KC, Tso EYK, Liu R, Chung TWH, Chu MY, *et al.* Triple combination of interferon beta-1b, lopinavir–ritonavir, and ribavirin in the treatment of patients admitted to hospital with COVID-19: an open-label, randomised, phase 2 trial. Lancet. 2020;395:1695–704.
8. Wang Y, Zhang D, Du G, Du R, Zhao J, Jin Y, *et al.* Remdesivir in adults with severe COVID-19: a randomised, double-blind, placebo-controlled, multicentre trial. Lancet. 2020;395:1569–578.
9. Xu X, Han M, Li T, Sun W, Wang D, Fu B, *et al.* Effective treatment of severe COVID-19 patients with tocilizumab. Proc Natl Acad Sci. 2020;117:10970–975.
10. FDA.gov [Internet] U.S. Food & Drugs Administration: Fact sheet for healthcare providers: emergency authorization for Paxlovid, [cited 2022 Feb 23]. Available from https://www.fda.gov/
11. Yang H, Yang M, Ding Y, Liu Y, Lou Z, Zhou Z, *et al.* The crystal structures of severe acute respiratory syndrome virus main protease and its complex with an inhibitor. Proc Natl Acad Sci. 2003;100:13190–195.
12. Ren J, Zhang AH, and Wang XJ. Traditional Chinese medicine for COVID-19 treatment. Pharmacol Res. 2020;155:104743.
13. Felle ZR, Wijayanti MA, and Supargiyono. The effect of pandanus conoideus lamk extract to the serum level of TNF-α, IL-10 and parasitemia of plasmodium berghei infected in Mice. Trop Med J. 2013;3:39–47.
14. Tafor D, Djunaidi A, Wasityastuti W, and Solikhah EN. Tumor necrosis factor-alpha (TNF-alpha) and intercellular adhesion molecule-1 (ICAM-1) expression of plasmodium berghei infected swiss mice treated with red fruit (*Pandanus Conoideus* Lam) ethanol extract. Trop Med J. 2013;3:155–65.
15. Tambaip T, Br Karo M, Hatta M, Dwiyanti R, Natzir R, Nasrum Mas M, *et al.* Immunomodulatory effect of orally red fruit (Pandanus conoideus) extract on the expression of CC chemokine receptor 5 mRNA in HIV patients with antiretroviral therapy. Res J Immunol. 2018;11:15–21.
16. Umar, AbdK. Flavonoid compounds of buah merah (*Pandanus conoideus* Lamk) as a potent SARS-CoV-2 main protease inhibitor: *in silico* approach, Futur. J Pharm Sci. 2021;7:158.
17. Prieto-Martínez FD, Arciniega M, and Medina-Franco JL. Acoplamiento molecular: avances recientes y retos, TIP Rev. Espec. en Ciencias Químico-Biológicas. 2018;21:65–87.
18. Lin X, Li X, and Lin X. A review on applications of computational methods in drug screening and design. Molecules. 2020;25:1375.
19. Rachmania RA, Hariyanti H, Zikriah R, and Sultan A. Studi *In Silico* senyawa alkaloid herba bakung putih (*Crinum Asiaticum* L.) pada penghambatan enzim siklooksigenase (COX). Jurnal Kimia VALENSI. 2018;4:124–36.
20. Masone D, and Grosdidier S. Collective variable driven molecular dynamics to improve protein–protein docking scoring. Comput Biol Chem. 2014;49:1–6.
21. Childers MC, and Daggett V. Insights from molecular dynamics simulations for computational protein design. Mol Syst Des Eng. 2017;2:9–33.
22. Ahmed M, Sadek MM, Abouzid KA, and Wang F, *In silico* design: extended molecular dynamic simulations of a new series of dually

acting inhibitors against EGFR and HER2, J Mol Graph Model. 2013;44:220–31.
23. Shivanika C, Kumar D, Ragunathan V, Tiwari P, Sumitha A. Molecular docking, validation, dynamics simulations, and pharmacokinetic prediction of natural compounds against the SARS-CoV-2 main-protease. J Biomol Struct Dyn. 2022;40:585–611.
24. Krieger E, Koraimann G, Vriend G. Increasing the precision of comparative models with YASARA NOVA-a self-parameterizing force field. Proteins Struct Funct Genet. 2002;47(3):1–10.
25. Biovia. Dassault Systèmes, Discovery studio visualizer, V21.1.0.20298. San Diego, CA:Dassault Systèmes; 2020.
26. Douangamath A, Fearon D, Gehrtz P, Krojer T, Lukacik P, Owen CD. *et al*. Crystallographic and electrophilic fragment screening of the SARS-CoV-2 main protease. Nat Commun. 2020;11:5047.
27. Nugraha G, Istyastono EP. Virtual target construction for structure-based screening in the discovery of histamine H2 receptor ligands. Int J Appl Pharm. 2021;13:239–41.
28. Nugraha G, Pranowo HD, Mudasir M, & Istyastono EP. Virtual target construction for discovery of human histamine H4 receptor ligands employing a structure-based virtual screening approach. Int J Appl Pharm. 2022;14(4):213–18.
29. Lengauer T, and Rarey M. Computational methods for biomolecular docking. Curr Opin Struct Biol. 1996;6(3):402–6.
30. Nurhidayah M, Fadilah F, Arsianti A, Bahtiar A. Identification of Fgfr inhibitor as St2 receptor/interleukin-1 receptor-like 1 inhibitor in chronic obstructive pulmonary disease due to exposure to E-cigarettes by network pharmacology and a molecular docking prediction. Int J App Pharm. 2022;14:256–66.
31. Jin Z, Du X, Xu Y, Deng Y, Liu M, Zhao Y, *et al*. Structure of Mpro from SARS-CoV-2 and discovery of its inhibitors. Nature. 2020;582:289–93.
32. Meanwell NA. Synopsis of some recent tactical application of bioisosteres in drug design. J Med Chem. 2011;54(8):2529–91.
33. Kubitzki MB, and de Groot BL. Molecular dynamics simulations using temperature-enhanced essential dynamics replica exchange. Biophys J. 2007;92(12):4262–70.
34. Jung J, Kobayashi C, and Sugita Y. Optimal temperature evaluation in molecular dynamics simulations with a large time step. J Chem Theory Comput. 2018;15(1):84–94.
35. Hospital A, Goni JR, Orozco M, and Gelpi JL. Molecular dynamics simulations: advances and applications. Adv Appl Bioinform Chem. 2015;8:37–47.
36. Arora S, Lohiya G, Moharir K, Shah S, and Yende S. Identification of potential flavonoid inhibitors of the SARS-CoV-2 main protease 6YNQ: a molecular docking study. Digital Chinese Med. 2020;3:239–48.
37. Schneider G. "De novo molecular design". Weinheim, Germany: Wiley-VCH Verlag GmbH & Co; 2014.
38. Chaudhary N and Aparoy P. Deciphering the mechanism behind the varied binding activities of COXIBs through molecular dynamic simulations, MM-PBSA binding energy calculations and per-residue energy decomposition studies, J Biomol Struct Dyn. 2017;35(4):868–82.
39. Zhang QY, and Aires-de-Sousa J. Random forest prediction of mutagenicity from empirical physicochemical descriptors. J Chem Inf Model. 2007;47(1):1–8.
40. Pires DE, Blundell TL, and Ascher DB. pkCSM: predicting small-molecule pharmacokinetic and toxicity properties using graph-based signatures. J Med Chem. 2015;58(9):4066–72.

How to cite this article:
Ananto AD, Pranowo HD, Haryadi W, Prasetyo N. Flavonoid compound of red fruit papua and it derivatives against sars-cov-2 mpro: An *in silico* approach. J Appl Pharm Sci. 2024;14(12):090–097.